

H. Versmold
H. Kubetzki
S. Musa
V. Urban

Small-angle scattering without sample rotation

Received: 8 December 2003
Accepted: 19 April 2004
Published online: 22 December 2004
© Springer-Verlag 2004

H. Versmold (✉) · H. Kubetzki · S. Musa
Institut für Physikalische Chemie der
RWTH, 52062 Aachen, Germany
E-mail: versmold@pc.rwth-aachen.de

V. Urban
ESRF, 38043 Grenoble, France

Abstract In this contribution small-angle scattering from layered systems is considered. When a colloidal dispersion is stirred it usually decomposes into layers. There are two important questions concerning these layers: What is the structure *in* a layer? What is the stacking structure *between* such layers? For concentrated colloidal dispersions both these questions can be investigated by small-angle scattering experiments. It will become apparent that the answer is also important for technical applications. Both a theoretical description as well as an experimental verification are given in the paper.

Keywords Colloids · Order · Couette cell · Tangential scattering

Introduction

Small-angle scattering has been used by biologists and physicians [1, 2, 3, 4] as well as physicists and macromolecular chemists for structural investigations [1, 5, 6, 7, 8, 9, 10]. In this paper we consider small-angle scattering from monodisperse, charge-stabilized colloidal dispersions. Under shear, such dispersions usually decompose into layers [10, 11, 12, 13]. There are two important questions concerning these layers: What is the structure *in* a layer? What is the stacking structure *between* the layers?

In order to investigate the scattering from layers we consider Fig. 1. Here a typical situation of small-angle scattering is depicted. For elastic scattering the smaller the scattering angle the more the scattering is due to particles positioned in a plane orthogonal to the incident

beam. On one hand, we may use this spatial selectivity; on the other hand, we must be aware of the fact that nothing can be learned about stacking of the layers in the direction of the beam. If one is interested in this question a rotation of the sample or the beam direction is necessary. Tangential incidence to this layer (Fig. 2) causes a geometry normal to the one considered in Fig. 1. Now stacking of the layer can be studied.

A simple device to study the mentioned behavior available at most research centers is the Couette cell shown in Fig. 3. If the beam is directed radially it will be normal to the layers of the dispersion. The cell is commonly used in this mode. Alternatively one might choose the tangential mode. Still the information comes from particles in a plane perpendicular to the beam; the layered sample, however, is rotated by 90°. Despite the fact that the Couette cell is more than 100 years old, this

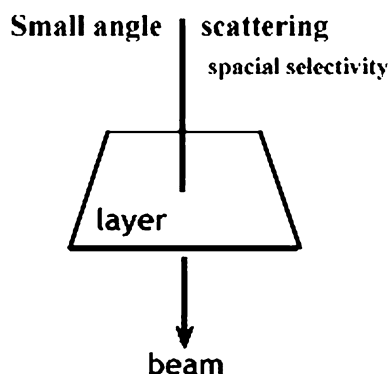


Fig. 1 Spatial selectivity: only layers perpendicular to the incident radiation contribute to small-angle scattering

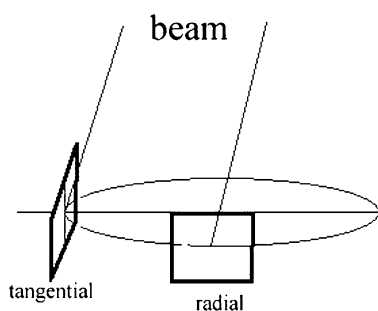


Fig. 2 Orientation of the particle layers for tangential and radial scattering of a Couette cell

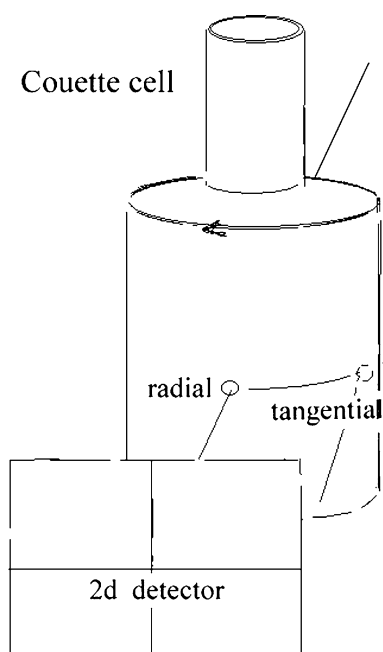


Fig. 3 Couette cell with indication of the positions for radial and tangential scattering

geometry has almost never been used. In the following sections we shall consider this tangential mode in more detail.

Theoretical

Solid-state concepts are useful to determine the scattering power along certain directions in reciprocal space. It is well known [5, 6] that for the occurrence of a Bragg reflection in atomic or molecular scattering the reciprocal lattice must be intersected by the Ewald sphere. The same principle holds for small-angle scattering from mesogenic systems. Usually, in an X-ray or a neutron scattering experiment the wave length λ of the radiation is much smaller than any distance a between colloid particles. Therefore the radius $R^* = 2\pi/\lambda$ of the Ewald sphere is huge compared with the reciprocal distance of the rods $a^* = 2\pi/a$ and as in Fig. 4 the sphere can be approximated by planes. In elastic small-angle scattering a given beam direction leads to a selection such that only particles belonging to a plain perpendicular to the beam contribute to the scattering in this direction. In Fig. 4 three planes are drawn; only one of them is perpendicular to the beam. By successively rotating the beam by angles α and/or β , the beam and/or the plane can be brought to one of the other positions (in our experiments both sample and flow but not the beam is rotated).

Next, Bragg scattering from a layered system will be considered. For this Miller indices h, k, l are introduced [5, 6]. The coordinate axes of the indices h and k are assumed to be in the layer of the layered sample, in which case the axis of l will be normal to the surface of the layers.

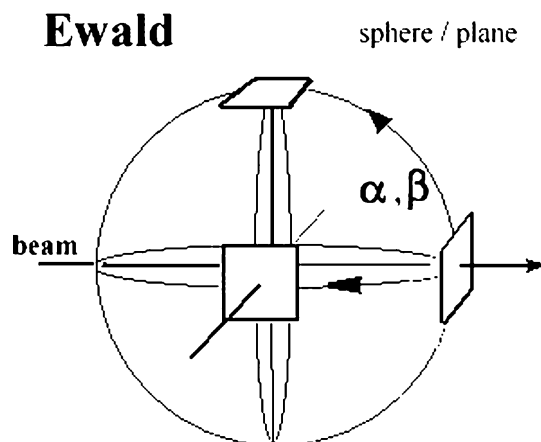


Fig. 4 View from the top on a (h,k) reciprocal layer of a shear-ordered colloidal system

Perpendicular scattering (radial scattering for the Couette cell)

Figure 5 presents an $l=0$ cut through a hexagonal h, k layer. This layer is part of the reciprocal space. The h, k layer is filled with black and white points. Black points belong to the totally symmetric representation of the layer. Depending on the handling of the l -dependence a point group or a space group description may be required. Let us begin with a flat hexagonal h, k layer. In this case a point group description with a degenerate e mode would be adequate. Energetically, the degenerate e levels are placed between two totally symmetric a levels.

By contrast, a space group description will be necessary if the l -dependence is taken into account. Now the degeneracy of the e mode is lifted. As described by Guinier [7, 8] for face-centered cubic (fcc) we have two separate levels. The previously degenerate reflections with maxima of the intensity at $l=n+1/2$, where n is a natural number, are now shifted to $l=n+1/2 \pm 1/6$. For the two stacking distributions, i.e., for ABCACBA... stacking and for the twin ACBACBA... stacking, the behavior on the corresponding white Bragg rods is shown in Fig. 6.

The step-by-step rotation method

This method has been used for years by physicists and chemists to determine the structure of crystals. We

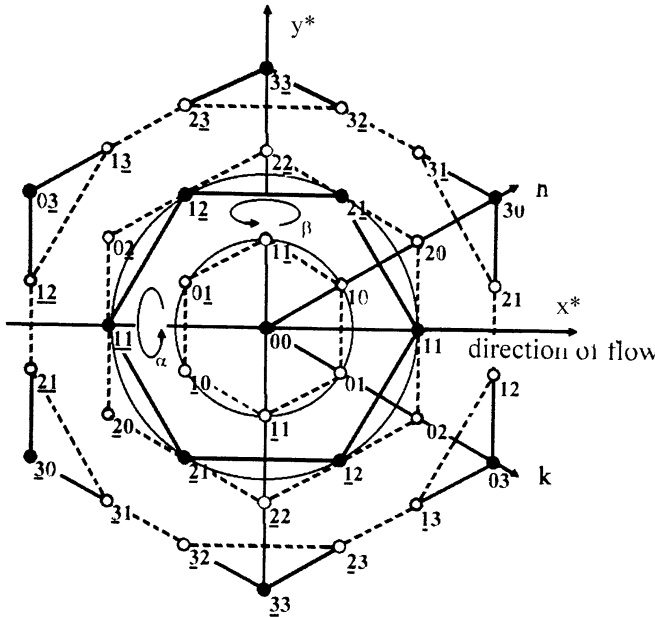


Fig. 5 An Ewald sphere becomes Ewald planes in small-angle scattering

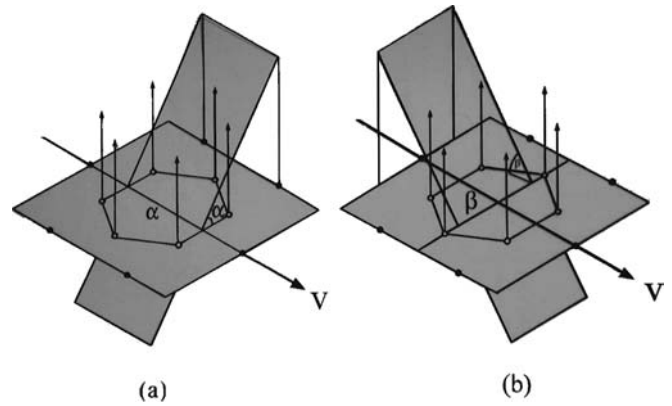


Fig. 6 α - and β -rotations of the Ewald planes in small angle scattering

consider Fig. 6 where the direction of flow V for ordering the sample and six directions in reciprocal space (Bragg rods of the first ring) are drawn. Depending on the angle α or β the tilted planes intersect the Bragg rods at various height and thus give the coordinates of the Bragg scattering intensity at the point of intersection. By rotating the sample plus flow by an angle α or β we are able to determine *step by step* the scattering intensity along the Bragg rods. This is the step-by-step method to determine the scattering intensity along a Bragg rod. There are two situations in which the proposed procedure does not work. For rods on the axis V we can choose the angle α as we always want the rod to be cut at $l=0$. A similar restriction holds for β rotations. In this case the intensity of rods on the β -rotation axis $(-1, 1; 0, 0; 1, -1)$ which is perpendicular to V cannot be determined by the step-by-step method. Fortunately, tangential scattering, to be described later, can be used in such cases.

Next, we consider an important result concerning the structure of fcc crystals which is also described in the book of Guinier [7]. The l -dependence of the intensity on the white Bragg rods is given by Fig. 7. For ABCACBA... stacking we have on the white rod $(h, k) = (1, -1)$ the behavior shown on the left-hand side of Fig. 7, where the open dot stands for the twin stacking ACBACBA... For the rod (h, k, l) we find a second white rod $(-h, -k) = (-1, 1)$ with the correct l -behavior shown on the right-hand side of Fig. 7. On the first rod the maxima of the intensity (filled dots) are at $l = 0.5 - 1/6; 1.5 - 1/6; \dots$, on the second at $l = 0.5 + 1/6; 1.5 + 1/6; \dots$, etc.

Tangential scattering (intensity determination without sample rotation)

In Fig. 8a the Ewald plane for perpendicular incidence ($\alpha = \beta = 0^\circ$) is shown. More interesting in the present

context is Fig. 8b with $\beta = 90^\circ$. Now all the rods on the axis perpendicular to V passing the center 0,0 are sliced along their length and the intensity along all the rods, i.e., their l -dependence, can be obtained simultaneously without rotation. This is a very efficient method to determine the intensity along a rod and is not mentioned in any of the well-known articles or books on colloid science [9, 10, 11, 12]. Since this tangential scattering, as it may be called, can be carried out with ordinary Couette cells available at most research centers it is to be

considered a very attractive method which has hardly been applied so far. Some experimental examples will be given in the next section.

Experimental results and discussion

The perpendicular and tangential scattering geometry which provide complementary information are shown for an oriented layer in Fig. 9 again.

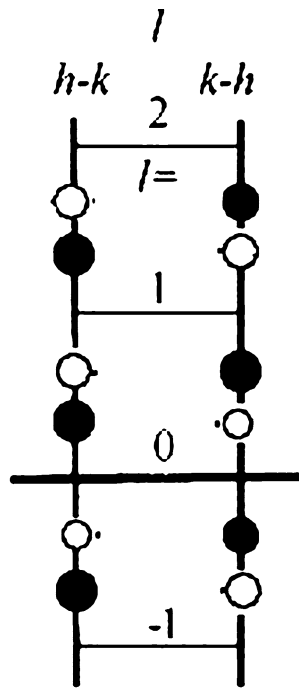


Fig. 7 Intensity on the rods $(h,k)=(-1,1)$ and $(-h,k)=(1,-1)$ for a face-centered-cubic (fcc) crystal

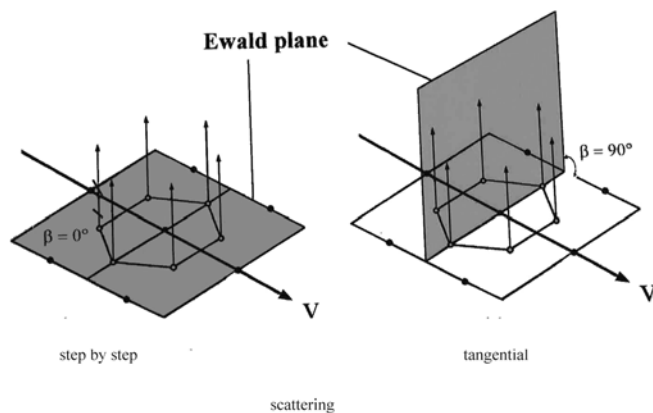


Fig. 8 Orientation of Ewald planes for perpendicular (radial for the Couette cell) and for tangential scattering

Perpendicular scattering (radial scattering for the Couette cell)

Although our perpendicular scattering data have already been published [13] we show them again in Fig. 10 for completeness. These data were obtained with our disk shear cell [14] for a charge-stabilized dispersion with particle diameter $\sigma = 94$ nm and a volume fraction of $\Phi = 34\%$ at rest after ordering the dispersion by shear. In Refs. [13, 14] the behavior of the dispersion in the viscoelastic range is shown, where rings were observed. The data were obtained at the ESRF beam line ID02 in Grenoble, France. The data to be shown in the next sections were obtained at the same beam line but with the Couette cell of that research center. The colloid material, however, was prepared and cleaned in Aachen.

Intensity along the rods: the step-by-step rotation method

With the Couette cell usually not a real rotation but a horizontal translation which is described in Refs. [15, 16] is performed and leads to an apparent β -rotation [13]. By translating the cell *step by step* apparent rotations are performed during which the Bragg rod is intersected at various heights by the Ewald plane. By measuring the scattering intensity for each new configuration, one is able to determine the l -dependence of the scattering intensity (i.e., the intensity along a rod). A typical result is shown in Fig. 5 of Ref. [13].

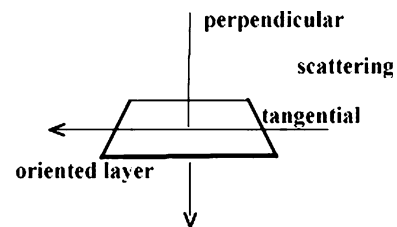


Fig. 9 Perpendicular and tangential scattering of an oriented layer

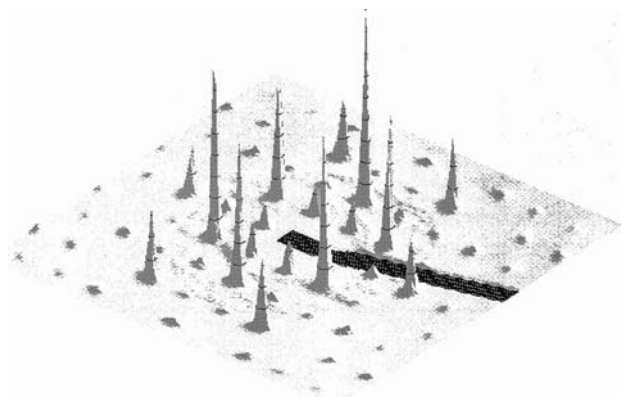


Fig. 10 Bragg reflections of layers as seen by perpendicular scattering (no stacking in this geometry obtainable)

Intensity along the rods: the tangential scattering method

The idea of tangential small-angle scattering is very simple: it is intended that the Bragg rods of a layered, oriented sample are sliced all the way (in the l direction) by the Ewald plane as in Fig. 8b. This way one obtains the whole l -dependence of several rods in a single experiment without rotation of the sample. We know of only two examples in which tangential scattering has been used. One is given in this paper. The second example is by Petukhov et al. These authors applied this technique with a completely different scattering cell and colloid while focusing on colloidal photonic crystals [17, 18]. Tangential scattering should be considered as a very efficient scattering method which allows the simultaneous determination of the scattering intensity along several black and white directions without sample rotation.

We begin the section with an experimental X-ray example. In Fig. 11 the fcc (single) crystal tangential Bragg scattering intensity of a concentrated dispersion is shown. The scattering pattern can be understood as follows. As outlined in the [Theoretical](#) section (Figs. 2, 8b) in tangential scattering the exciting beam and the flow V which was used to order the dispersion point in the same direction. As a result the Bragg rods are sliced by the Ewald plane and we have a continuous intensity distribution with a maximum in the center of a layer. Thus, the distance from maximum to maximum equals the distance c^* from one reciprocal layer to the next one. This is the behavior for the black spots. Slightly different behavior is observed for the white rods. For a single crystal we do *not* expect the reflections to occur at $l=0.5; 1.5 \dots$. But there are two types of rods: for the first type we have maxima at $l=0.5-1/6; 1.5-1/6 \dots$, whereas for the second type we have them at $l=0.5+1/6; 1.5+1/6 \dots$. It is interesting to note that the height of the stores is $l=c^*$ for both types of white rods and for the black

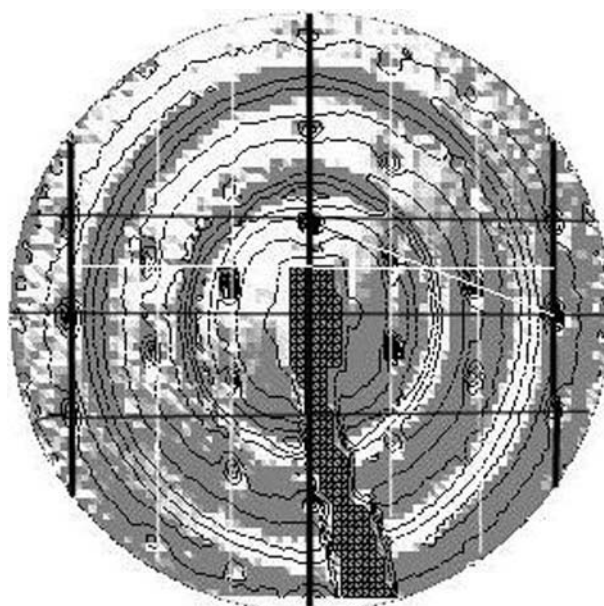


Fig. 11 Slow exchange between layers of a fcc single crystal (concentration 30 vol%)

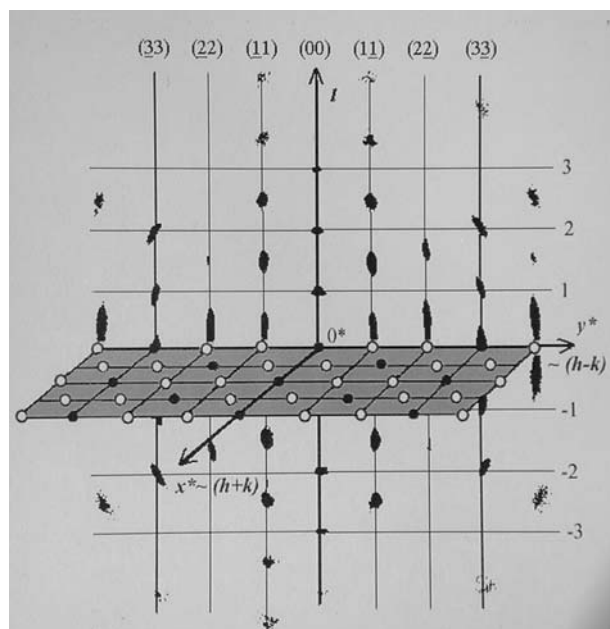


Fig. 12 Summary of the experiments in perpendicular and in tangential geometry. The data of Fig. 10 were used to determine the h,k distribution in the layer. The l -dependence of the X-ray scattering intensity as obtained by tangential scattering is given at the *back*. Functions similar to the radial distribution function of liquids can be calculated but are not shown here

spots. Thus the height of the stores can be determined from either type.

In Fig. 12 our synchrotron X-ray experiments performed with the sample at rest are summarized. In the

layers a hexagonal structure was observed as described in Ref. [13]. The layering of the fcc structured concentrated dispersion is demonstrated by tangential scattering, shown at the back in Fig. 12. Starting at the origin 0^* in reciprocal space we have the rectangular axes $x^* \sim (h+k)$, $y^* \sim (h-k)$ and $z^* \sim l$. In the y^* direction a clear ...black-white-white-black... sequence of the rods is visible in Fig. 12. Further, a shift of $\Delta l = 1/2 \pm 1/6$ of the maxima on the white rods relative to the black spots

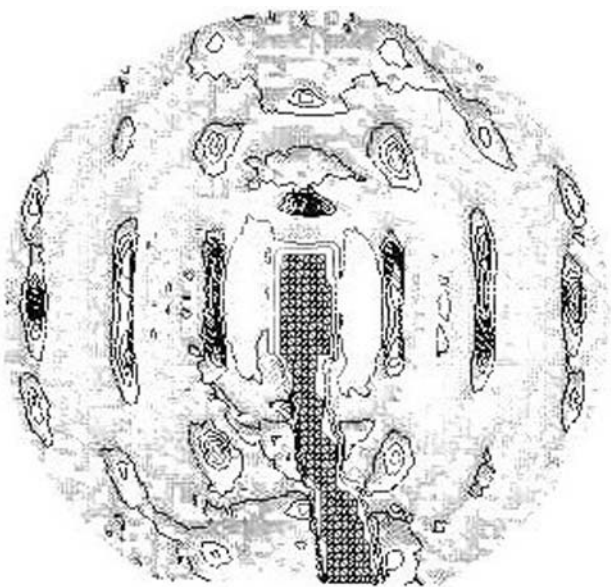


Fig. 13 Intermediate exchange rate between layers of a fcc crystal due to screening of the potential (limitation of the range of interaction)

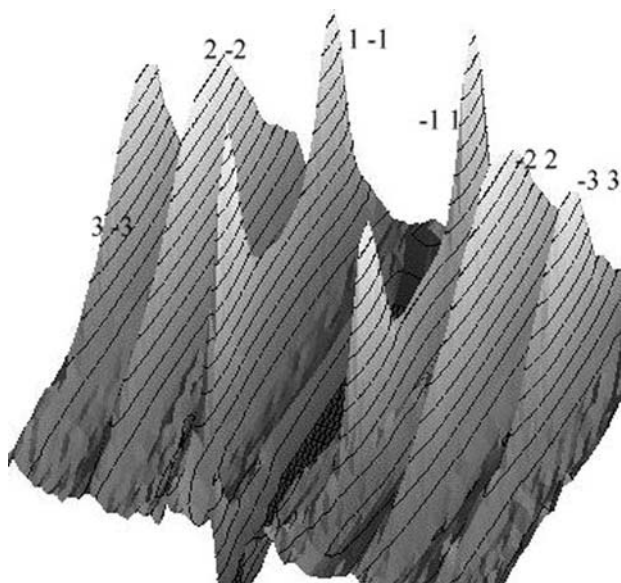


Fig. 14 Forced exchange between layers due to the shear rate

can be seen as predicted in the Theoretical section. In contrast to earlier investigations [19, 20], we distinguish between black and white directions in reciprocal space.

Tangential scattering could be altered by exchange phenomena. As in NMR spectroscopy, lines can be shifted or they may even collapse to a single line. This behavior can be used to investigate the stacking kinetics. For example, a layered state can be shorter-lived owing to spontaneous or to forced exchange processes. We show one example for spontaneous and one for forced exchange. The spontaneous exchange, Fig. 13, was achieved by adding a certain amount of electrolyte (KCl) to the dispersion. The limitation of the range of interaction of the charge-stabilized dispersions causes an increase of the exchange rate of the layers and the scattering pattern shown in Fig. 13 was observed. This is to be compared with Fig. 11 where for the same sample, without salt, a slow exchange is observed.

The experiments shown so far were carried out at rest after ordering the samples by shear. For the forced exchange experiment to be described next the sample was continuously in motion. In the case shown (Fig. 14) the shear rate was increased until the doublet on the white rods (2,-2) and (-2,2) disappeared. It should be noted that the doublet on the white rods (1,-1) and (-1,1) is still clearly visible.

Conclusion and summary

Small-angle scattering of X-rays and neutrons is at present a method widely used with quite different

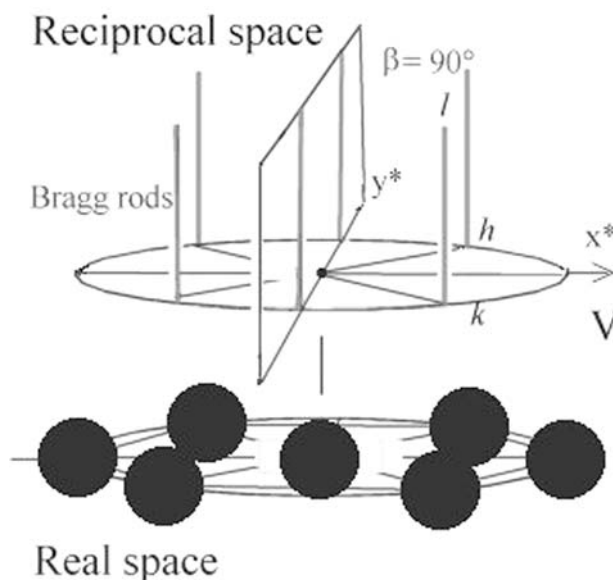


Fig. 15 Comparison of real and reciprocal space of a layered sample

intentions by biologists, physicians, physicists and chemists. Biologists and physicians are mainly interested in the pair distance distribution function, which for isotropic scattering gives information on the position of active centers in proteins. Considerably more information would be obtainable if the anisotropic part of the scattering were also considered. This is commonly done by solid-state physicists, chemists, and crystallographers who collect their data by sample rotation. In the present paper we have shown that this is not necessary in all cases. By using tangential scattering in small-angle scattering the intensity along several Bragg rods can be obtained simultaneously without rotation of the sample.

In Fig. 15 an explanation and a summary of the data shown in this paper and in particular in Fig. 12 are given. If a monodisperse concentrated dispersion is

subjected to shear flow it usually decomposes into layers. Figure 15 refers to such a situation. In the lower part of Fig. 15 a particle layer in real space is drawn. In the layer we have the hexagonal symmetry typical for charge-stabilized dispersions. The reciprocal space of the hexagonal particle layer is drawn in the upper panel. It consists of hexagonally arranged Bragg rods which are perpendicular to the original layer but rotated by 90°. For a single layer the intensity along the rods is uniform as indicated in Fig. 15. For a fcc dispersion it is modulated as shown in Figs. 11, 12 and 13.

Acknowledgements Financial support of the Deutsche Forschungsgemeinschaft and the Fonds der Chemischen Industrie is gratefully acknowledged.

References

1. Lindner P, Zemb T (eds) (1991) Neutron, X-ray and light scattering: introduction to an investigative tool for colloidal and polymeric systems. North-Holland, Amsterdam
2. Guinier A, Fournet G (1955) Small-angle scattering of X-rays. Wiley, New York
3. Glatter O, Kratky O (eds) (1982) Small angle X-ray scattering. Academic, London
4. Feigin LA, Svergun DI (1987) Structure analysis by small-angle X-ray and neutron scattering. Plenum, New York
5. Kittel C (1967) Introduction to solid state physics. Wiley, New York
6. Altman SL (1994) Band theory of solids: an introduction from the point of view of symmetry. Oxford University Press, Oxford
7. Guinier A (1963) X-ray diffraction. Freeman, London
8. Paterson MS (1952) J Appl Phys 23:805
9. Pusey PN (1991) In: Hansen JP, Levesque D, Zinn-Justin J (eds) Liquides, crystallization et transition vitreuse, Les Houches 1989, vol II. North-Holland, Amsterdam, p 763
10. Ackerson BJ (1987) In: Safran SA, Clark NA (eds) Physics of complex and supermolecular fluids. Wiley, New York, p 553
11. van de Ven TGM (1989) Colloidal hydrodynamics. Academic, London
12. (a) Hunter RJ (1994) Introduction to modern colloid science. Oxford Science, Oxford; (b) Hunter RJ (1987) Foundations of colloid science, vols I, II. Oxford Science, Oxford
13. Versmold H, Musa S, Bierbaum A (2002) J Chem Phys 116:2658
14. Versmold H, Musa S, Dux C, Lindner P, Urban V (2001) Langmuir 17:6812
15. Ackerson BJ, Hayter JB, Clark NA, Cotter L (1984) J Chem Phys 84:2344
16. Ashdown S, Markovic I, Ottewill RH, Lindner P, Oberthür RC, Rennie AR (1990) Langmuir 6:303
17. Petukhov AV, Dolbnya IP, Aarts DGAL, Vroege GJ, Lekkerkerker HNW (2003) Phys Rev Lett 90:2834
18. Dolbnya IP (2004) Thesis. University of Utrecht
19. Loose W, Ackerson BJ (1994) J Chem Phys 101:7216
20. Clarke SM, Rennie AR, Ottewill RH (1997) Langmuir 13:1964